

Article

Composition Component Influence on Concrete Properties with the Additive of Rubber Tree Seed Shells

Alexey N. Beskopylny ^{1,*}, Evgenii M. Shcherban' ², Sergey A. Stel'makh ³, Besarion Meskhi ⁴,
Alexandr A. Shilov ³, Valery Varavka ⁵, Alexandr Evtushenko ³, Yasin Onuralp Özkılıç ⁶, Ceyhun Aksoyly ⁷
and Memduh Karalar ⁸

¹ Department of Transport Systems, Faculty of Roads and Transport Systems, Don State Technical University, 344003 Rostov-on-Don, Russia

² Department of Engineering Geology, Bases, and Foundations, Don State Technical University, 344003 Rostov-on-Don, Russia

³ Department of Unique Buildings and Constructions Engineering, Don State Technical University, 344003 Rostov-on-Don, Russia

⁴ Department of Life Safety and Environmental Protection, Faculty of Life Safety and Environmental Engineering, Don State Technical University, 344003 Rostov-on-Don, Russia

⁵ Research and Education Center "Materials", Don State Technical University, 344003 Rostov-on-Don, Russia

⁶ Department of Civil Engineering, Faculty of Engineering, Necmettin Erbakan University, 42000 Konya, Turkey

⁷ Department of Civil Engineering, Faculty of Engineering and Natural Sciences, Konya Technical University, 42075 Konya, Turkey

⁸ Department of Civil Engineering, Faculty of Engineering, Zonguldak Bulent Ecevit University, 67100 Zonguldak, Turkey

* Correspondence: besk-an@yandex.ru; Tel.: +7-8632738454



Citation: Beskopylny, A.N.; Shcherban', E.M.; Stel'makh, S.A.; Meskhi, B.; Shilov, A.A.; Varavka, V.; Evtushenko, A.; Özkılıç, Y.O.; Aksoyly, C.; Karalar, M. Composition Component Influence on Concrete Properties with the Additive of Rubber Tree Seed Shells. *Appl. Sci.* **2022**, *12*, 11744. <https://doi.org/10.3390/app122211744>

Academic Editor: Dario De Domenico

Received: 27 October 2022

Accepted: 16 November 2022

Published: 18 November 2022

Publisher's Note: MDPI stays neutral with regard to jurisdictional claims in published maps and institutional affiliations.



Copyright: © 2022 by the authors. Licensee MDPI, Basel, Switzerland. This article is an open access article distributed under the terms and conditions of the Creative Commons Attribution (CC BY) license (<https://creativecommons.org/licenses/by/4.0/>).

Abstract: The growth in the volume of modern construction and the manufacture of reinforced concrete structures (RCSs) presents the goal of reducing the cost of building materials without compromising structures and opens questions about the use of environmentally friendly natural raw materials as a local or full replacement of traditional mineral components. This can also solve the actual problem of disposal of unclaimed agricultural waste, the features of which may be of interest to the construction industry. This research aimed to analyze the influence of preparation factors on concrete features with partial substitution of coarse aggregate (CA) with rubber tree (RT) seed shells and to determine the optimal composition that can make it possible to attain concrete with improved strength features. CA was replaced by volume with RT seed shells in an amount from 2% to 16% in 2% increments. Scanning electronic microscopy was employed to investigate the structure of the obtained concrete examples. The maximum increase in strength features was observed when replacing coarse filler with 4% RT seed shell by volume and amounted to, for compressive and axial compressive strength (CS) and tensile and axial tensile strength (TS) in twisting, 6% and 8%, respectively. The decrease in strain features under axial compression and under axial tension was 6% and 5%, respectively. The modulus of elasticity increased to 7%. The microstructure of hardened concrete samples with partial replacement of CA with RT seed shells in the amount of 2%, 4% and 6% was the densest with the least amount of pores and microcracks in comparison with the structure of the sample of the control composition, as well as samples with the replacement of CA with RT seed shells in an amount of more than 6%. The expedient effective replacement of CA with RT shells led to a reduction in battered stone of up to 8%.

Keywords: rubber tree seed shell; concrete; coarse aggregate; strength features; strain features

1. Introduction

1.1. Background

Concrete and RCSs occupy one of the main roles in modern construction around the world, the growth in the pace and volume of which is inevitably associated with an

increase in the need for raw materials and construction materials for structures and buildings [1,2]. The traditional mineral components of the concrete mixture are non-renewable resources, which, despite their large number, raise the question of the relevance of their local replacement with natural and renewable counterparts. An increase in the production of RCSs makes relevant the search for ways to reduce cost, which can be quite high [3–6]. At the same time, the growing volume of production processes within the agricultural industry entail an increase in the amount of waste, most of which, despite potentially interesting properties, is not employed, which opens up the question of finding promising methods of use. All of the above indicates the need to develop environmentally friendly concrete, in which traditional mineral components are locally or completely replaced by natural analogues, including agricultural waste. This approach can make it possible to achieve environmentally friendly concrete with a reduced cost, while having improved strength features compared to conventional concrete [7,8]. Many wastes from the agricultural industry have strength features comparable to the mineral components of concrete and can be successfully used in the construction industry. One of the promising natural materials is rubber seed shells (RSSs). The RT (*Hevea brasiliensis*) is cultivated mainly in Indonesia, Thailand, India, Vietnam, Nigeria, Myanmar, Sri Lanka, Cambodia, Congo, Malaysia, Liberia and Brazil [9,10]. It is of interest due to the high content of rubber in the milky sap of this plant (about 40–50%), which makes it an essential raw material for the global manufacturing of natural rubber. In addition, the whey produced in the process of coagulation and separation of rubber from latex contains proteins in an amount of 0.6%, which makes it suitable for animal feeding [11–15]. The seeds of the plant are employed for cultivation but also contain about 35–37% drying oil. The fruit of the RT is a hard, three-leaved pod (shell) containing three hard-shelled, ovoid seeds (Figure 1).

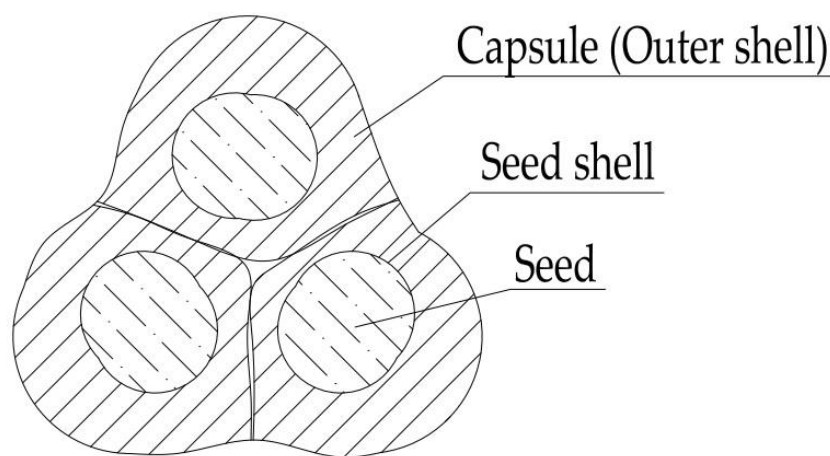


Figure 1. The assembly of the fruit of the RT.

The fruits look like chestnuts; they are dark brown, round, three-leaved boxes with a smooth shell, 2–3 cm in size. The seeds are small and ovoid, about 3 mm in diameter, with juicy cotyledons containing up to 40% fatty oil. Ripe leaves open, fall into the soil, and under favorable weather conditions begin to germinate in a few weeks. The shell of the RT, despite its outstanding strength features, is the only unemployed and non-utilized part of the plant, which lies on the ground in large quantities and decomposes [16–22]. The water absorption of the RT shell is 20–30%. The relatively high renewability and low susceptibility to decay of this raw material creates an urgent need for its disposal in the agricultural industry. Combustion of such material is impractical due to high CO₂ emissions into the atmosphere [23–26]. The foregoing confirms the significant potential of using RT seed shells as a partial replacement for CA both for construction, due to its outstanding strength features, and for the agricultural industry due to the lack of well-studied and environmentally friendly technologies for its disposal [27–32]. In addition, local replacement of CA in concrete with RT seed shells can significantly reduce the cost

and weight of such a composition, which makes the presented technology attractive for the needs of modern construction [33–39]. However, despite this, studies considering the local or complete replacement of CA in concrete with the shells of RT seeds are extremely few due to the low prevalence of this plant and the lack of stable links between the rubber and construction industries [40,41].

One study [40] considered the local replacement of coarse concrete aggregate with battered RT seed shells. Compositions with the addition of natural raw materials in the amount of 5%, 10%, 15% and 20% of the volume of concrete were considered. The cubic strength of concrete in compression and TS in twisting were studied. The consequences achieved were compared with the control composition, consisting of ordinary concrete, not containing the shell of the seeds of the RT. The consequences of this study presented that the compressive strength and TS of concrete in twisting when replacing CA with RT seed shells by more than 10% of the volume of concrete decreased in direct proportion to the amount of RT seed shells. When replacing CA with a natural analogue in an amount of less than 10%, the decrease in the studied strength features was insignificant and suitable for the needs of modern construction. In this study, only two strength parameters of concrete were considered, and the factor of reducing the weight of concrete and changing its heat-conducting properties was not considered. In ref. [41], the features of self-compacting concrete were considered with the complete replacement of CA with RT shells, covered by vulcanization with two layers of latex, while varying the ratio of cement, sand, and crushed stones. The mobility of the resulting mixture and cubic strength of concrete were considered. According to the consequences of the study, it was revealed that the ratio cement:sand:coarse aggregate equal to 1:0.94:0.046 is optimal. This study considered only one strength parameter and did not consider the weight of the resulting composition.

The study [42] adds to the growing body of literature on solutions to problems associated with integral bridge fills. The results obtained in this paper and other physics models and field instruments for mixed tire and soil backfill suggest a new side ground pressure coefficient for integral bridges based on the tire content and mixing area with the wall. Recycling tire rubber in soil mixtures significantly reduces the stress factor, earth equivalent peak pressure factor and settlement after 120 cycles [42]. The use of waste rubber tires in concrete is still scattered and unclear. Consideration in ref. [43] of important areas of concrete freshness, durability and strength properties, as well as microstructures, is promising. However, there are certain obstacles that prevent the use of such waste as aggregate in large quantities, such as the poor structural strength of rubber and poor bonding to the cement matrix. Rubber, however, exhibits mechanical strength comparable to reference concrete, up to 20% [43].

The study [44] was carried out to fill an existing gap in the literature on the evaluation of the compressive strength of concrete containing binary additional cementitious materials. The effect of different substitution levels of three different common pozzolans (metakaolin, zeolite, and fly ash) in concrete mixes was studied. The optimal level of substitution for the design of binary mixtures was 10% by weight of cement. The developed model for predicting the compressive strength of concrete containing binary additional cementitious materials had an accuracy in terms of MSE of 0.0017 for the validation data. In addition, more than 42% and 94% of the data were predicted with an error of less than 2% and 10%, respectively. The effect of various combinations of additional cementing materials with any arbitrary chemical composition at any age from 3 to 365 days can be predicted with high accuracy using the MLP network proposed in [44].

Of no small importance are the indicators of the durability of rubber concrete, which depend on the content of rubber in concrete and the method of pre-treatment of rubber [45–48]. It has been established that rubber has promising characteristics for increasing the durability of concrete; the addition of rubber can reduce the diffusion of chlorides and slow down the corrosion of steel, and during transportation, sodium and chloride ions are retained in rubber chains [45].

In accordance with the foregoing, a certain gap in the field of knowledge has been identified regarding the accumulation and systematization of theories and experimental data on functional concretes with a mineral binder using aggregates of plant origin. The ongoing study is intended to eliminate this gap in terms of studying the compatibility of the initial components of mineral and plant origin, the features of the structure formation of such composites and the relationship at the micro and macro levels according to the fundamental principle of concrete science “composition — structure — properties”.

1.2. Rationale

The novelty of the study is as follows:

- (1) For the first time, the properties of concrete using the RT seed shell were investigated in terms of TS in twisting, deformability and other structural features, which has not been previously performed and is not known in the literature;
- (2) We present the development of a concrete formulation modified by local replacement of CA with RT seed shells to improve concrete performance;
- (3) As a result of the theoretical and experimental studies, the relationship between the initial recipe–technological parameters and the indicators of the resulting concretes based on the shell of the RT seeds was determined.

The present study develops the theme of “green concrete”, which implies the local or complete replacement of traditional concrete components with vegetable analogues, which are agricultural waste [49–54]. In our case, a local replacement of large aggregate (battered stone) in the composition of concrete is performed with the shell of the seeds of an RT. The shell is additionally limited to mechanical processing until a certain size modulus is reached to improve features of the strength of concrete, as well as to ensure its uniformity.

1.3. Research Significance

The conducted research is a scientific milestone, involving the systematization and development of existing theories of hardening of concrete composites based on agricultural waste, the processes of their structure formation at the micro and macro level, and the formation of their properties. From an applied point of view, we hypothesized, tested and proven experimental positions on the interdependence between the compositions, structure and properties of such concretes. Thus, the significance of this research is of a complex theoretical and applied nature and can be used by researchers and engineers.

2. Materials and Methods

During the experimental investigations, Portland cement of the CEM I 42.5N brand (Novoroscement, Novorossiysk, Russia) was used without additives. The main components and features of cement were as indicated in ref. [51].

Battered sandstone (“Repnyanskoye quarry management”, Chistoozerny village, Russia) was employed as a thick aggregate with the following physical and mechanical features: fraction size 5–20 mm; bulk density 1428 kg/m³; true density 2560 kg/m³; crushability 13.8% by weight; content of lamellar and needle-shaped grains 7.2 wt.%; voidness 43%.

Quartz sand (Arkhipovsky quarry, Arkhipovskoye village, Russia) was employed as a fine aggregate with the properties as specified in ref. [51].

As a natural CA for local replacement of battered stone, the shell of the seeds of an RT from Malaysia was employed. The shell was dried in a ShS-80-01 SPU oven (Smolenskoye SKTB SPU, Smolensk, Russia) and battered in a ShD-6 lab jaw crusher (Vibrotechnik, St. Petersburg, Russia) to a fraction size of 5–20 mm. The method for obtaining ready-made CA based on the shell of the seeds of the RT is indicated in Figure 2.

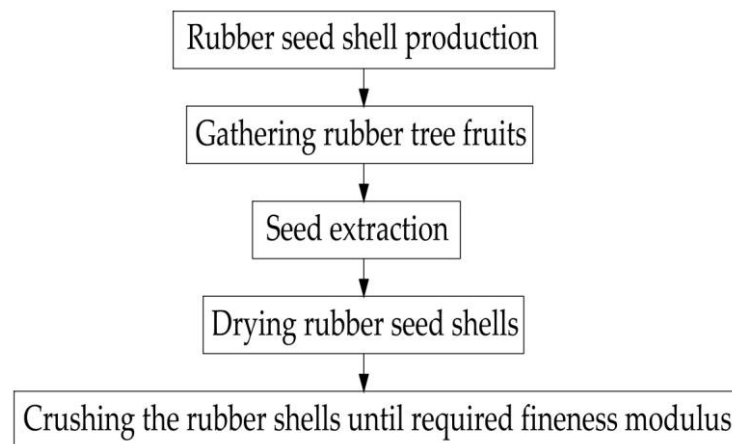


Figure 2. Method for obtaining CA based on the shell of the seeds of the RT.

The proportion of the mixture was as follows. Portland cement:water:sand:crushed stone—1:0.57:2.25:3.21. The workability of the mixture corresponded to the draft of a standard cone with a height of 300 mm, a large diameter of 200 mm and a small diameter of 100 mm, equal to 5–9 cm.

The preparation of concrete mixtures was performed in a lab BL-10 (“ZZBO”, Zlatoust, Russia). To compress the mixture during the molding of the samples, a regular lab vibrating stage SMZh-539-220A (IMASH, Armavir, Russia) was chosen; the time was 60 s for vibration. The sample preparation procedure included the following main technological steps (Table 1).

Table 1. Sample preparation procedure.

Technological Operation	Description
Dosing	At the dosing stage, the concrete components were measured; the components were weighed on a VLTE-2100 balance (NPP Gosmetr, St. Petersburg, Russia). The accuracy is 0.05 g.
Loading concrete mix components	The components were loaded into the concrete mixer in the following order: water, cement, additive, sand, CA (battered stone and RT seed shell).
Mixing	The components were mixed in the concrete mixer until a homogeneous mass was obtained.
Molding	The mixture was poured into sample molds, then formed on the laboratory vibratory platform and compressed to the desired state.
Storage	The samples were placed in a normal hardening chamber, where they were kept for 1 day; then, they were removed from the molds and hardened for another 27 days.

After curing for 28 days in a normal hardening chamber, the samples were tested on an IP-1000 hydraulic press and a R-50 tensile experiment machine.

Concrete strength control and evaluation were performed in accordance with GOST 18105 [55].

A study of the structure of hardened concrete samples with local replacement of CA with RT seed shells was performed using a ZEISS CrossBeam 340 electron microscope.

In total, 1 series of samples of the control composition and 8 series of samples with different amounts of RT seed shells were made and tested. The experimental research program is indicated in Figure 3.

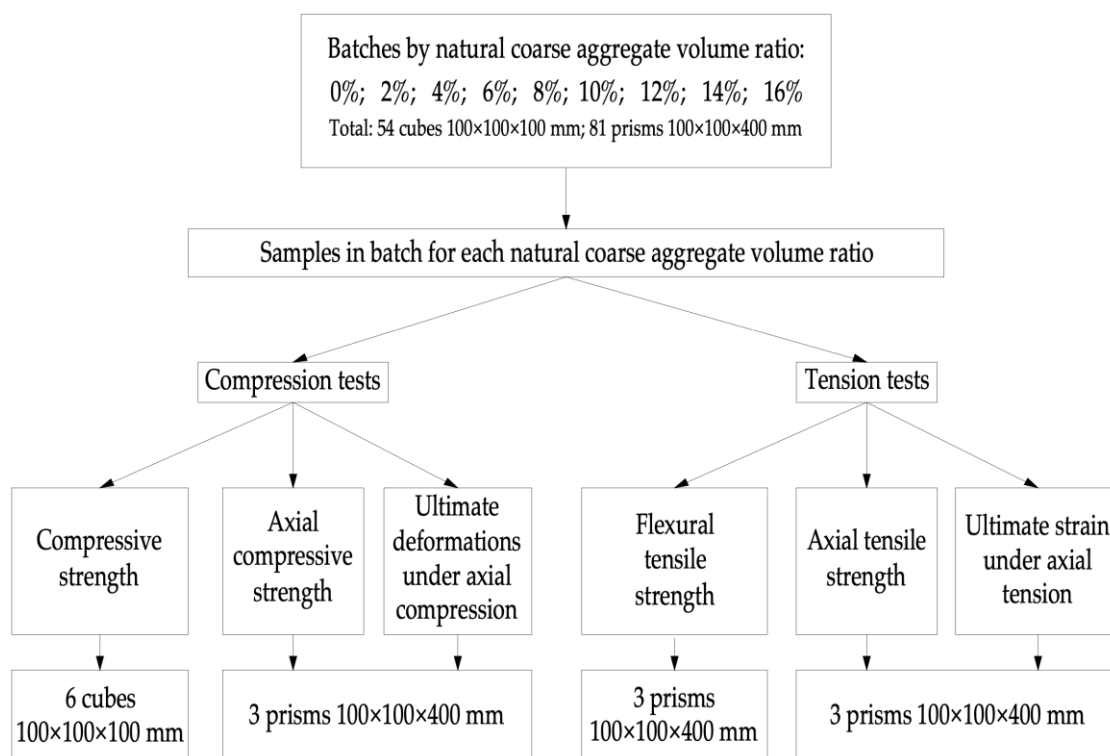


Figure 3. The program of investigations of the influence of local replacement of CA with RT seed shells on the strength–strain features of concrete.

Flexural compressive and TS experiments were performed in accordance with GOST 10180 [56]. Prismatic strength was determined according to the standard GOST 24452 [57]. Also in this investigation study, measuring “devices were employed: metal measuring ruler was selected as 500 mm; device for gauging deviations from the plane NPL-1; device for gauging deviations from perpendicularity NPR-1” [58–60].

Determining the defects in the form of cracks, ribs, crusts and debris was limited to visual inspection in the experiment. Samples with cracks, rib holes with a depth of more than 10 mm, shells with a diameter of more than 10 mm and a depth of more than 5 mm, as well as traces of delamination and under compaction of the concrete mix were not subject to experiment. Reference surfaces were chosen as noticeable on the samples to which forces were operative through loading. The supportive surfaces of the molded cubes planned for the compression experiment were selected. Thus, throughout the test, the compressive force was activated. Before placing the sample on the press, the concrete elements enduring from the earlier test on the base plates of the experimental machine were removed. The specimens were loaded continuously at a constant rate of load rise until their failure. The load time until the sample was destroyed was at least 30 s. The highest force obtained during the test was determined as the breaking load. The destroyed sample was limited to visual inspection. The top plate of the test machine was aligned, for example, with the upper support face, and the planes were adjacent to one another. The sample was loaded at a constant load increase rate of (0.6 ± 0.2) MPa/s [56].

For a tensile test in twisting, a prism sample was placed on a press and loaded at a constant load increase rate of (0.05 ± 0.01) MPa/s. If the specimen did not fail in the middle third of the span, or if the fracture plane of the specimen was inclined to the vertical plane by more than 15° , then this test result was not taken into consideration while defining the average strength of the concrete of a series of samples [56].

In the axial tensile test, the sample was fixed in a tensile experiment machine and loaded to failure at a continuous rate of load rise of (0.05 ± 0.01) MPa/s. The examination results were not considered if the obliteration of the sample did not take place in the

operational area or the flat surface of obliteration of the sample was disposed more than 15° to its horizontal axis [56].

The CS of concrete conflict of interest $R_{b.cub}$ was determined with an exactitude of 0.1 MPa using Equation (1):

$$R_{b.cub} = \alpha \frac{F}{A} \quad (1)$$

The TS of concrete in twisting R_{btb} was determined with an accuracy of 0.01 MPa using Equation (2):

$$R_{btb} = \delta \frac{Fl}{ab^2} \quad (2)$$

The axial TS of concrete R_{bt} was calculated with an accuracy of 0.01 MPa using the following formula:

$$R_{bt} = \beta \frac{F}{A} \quad (3)$$

where α , δ , β are scale factors; F is the breaking load, N; A is the area of the working section of the sample, mm^2 ; l is the span size between the supports; a and b are characteristic dimensions of the prism.

When determining the modulus of elasticity, the press force-meter scale was chosen, and the anticipated assessment of the breaking load P_{ult} was set as 70% to 80% of the maximum permitted by the nominated scale. When determining the prism strength, the scale of the force meter was chosen in accordance with the requirements of ref. [56]. Prior to experimentation, the alignment of the sample initial reading with the instruments was tested by dividing the instrument scale. As a result, the initial compression force, taken as the limiting zero in tests, could not be more than 2% of the breaking force. The value of the anticipated breaking load of the samples during the experiment was established according to the CS of cube samples made from one batch, determined in accordance with GOST 10180 [56]. The ratio for the same sections of cubes and prisms occupied 80 to 90% of the average refractive load of the cube samples [57].

While defining the prismatic strength and modulus of elasticity, the loading of the sample to a force level equivalent to $(40 + 5)\% P_{ult}$ was achieved in stages equivalent to 10% of the predictable breaking force, while maintaining the rate (0.6 ± 0.2) MPa/s within individual steps. At each phase, the load was maintained for 4 to 5 min (when heated, up to 15 min) and analyses were recorded on the devices at the start and at the finish of the exposure of the load phase. At a load equal equivalent to $(40 \pm 5)\% P_{ult}$, the devices were removed from the sample. After removal of the devices, further loading of the sample was performed constantly at a continuous ratio following GOST 10180 [53,57].

The prismatic strength R_{pr} is considered for each example using the following formula:

$$R_{pr} = \frac{P_{ult}}{F} \quad (4)$$

where P_{ult} is the collapsing force measured on the gauge strength measure; F is the cross-sectional area of the example, determined by its linear dimensions according to GOST 10180.

The modulus of elasticity E was considered for each sample at a load level of 30% of the breaking load, according to the following formula:

$$E = \frac{\sigma_1}{\varepsilon_{1y}} \quad (5)$$

where $\sigma_1 = P_1/F$ is the stress increment from conditional zero to the level of external load equal to 30% of the breaking load; P_1 is the corresponding increment of the external load; ε_{1y} is the increment of the elastic-instantaneous relative longitudinal deformation of the example, corresponding to the load level $P_1 = 0.3P_{ult}$ and measured at the beginning of

each stage of its application. Within the loading stage, the deformations were determined by linear interpolation.

The value of ϵ_{1y} was determined by the following formula:

$$\epsilon_{1y} = \epsilon_1 - \sum \epsilon_{1i} \tag{6}$$

where ϵ_1 is the increment of the total relative longitudinal and transverse deformations of the example, corresponding to the load level $P_1 = 0.3P_{ult}$ and restrained at the end of the stage of its application; $\sum \epsilon_{1i}$ is the increment of relative longitudinal and transverse strains of rapid creep, achieved by holding the load at the loading stages up to the load level $P_1 = 0.3P_{ult}$.

The increment of relative longitudinal and transverse strains was calculated as the arithmetic mean of instrument readings over four prism faces [57].

3. Results

3.1. Investigation of the Influence of the Amount of Added RSS instead of CA on the Strength–Strain Features of Concrete

The consequences of the influence of local replacement of CA with RT seed shells on the strength of concrete are indicated in Figures 4–7.

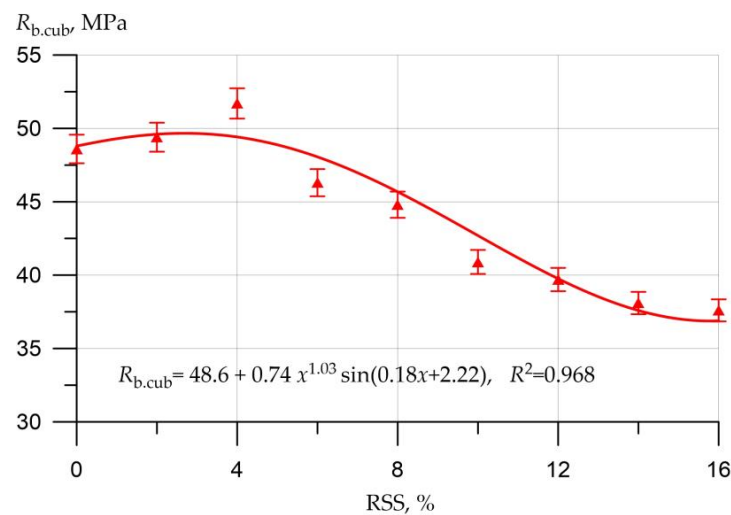


Figure 4. The influence of local replacement of CA with RT seed shells on CS $R_{b,cub}$.

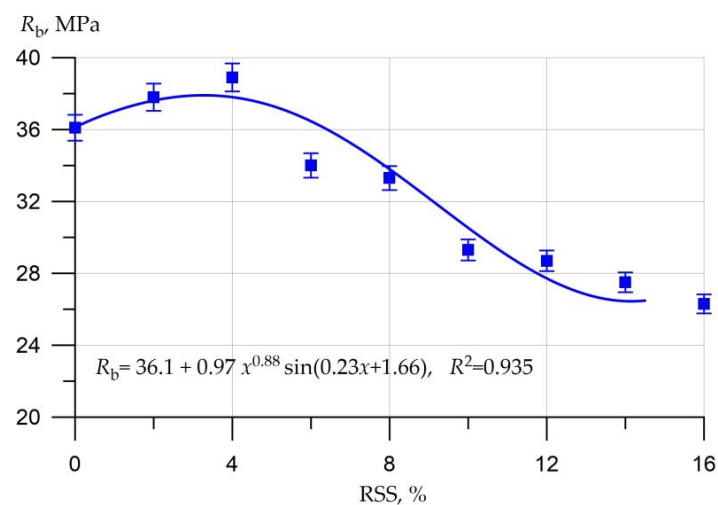


Figure 5. Results of investigational studies of the influence of local replacement of CA with RT seed shells on axial CS R_b .

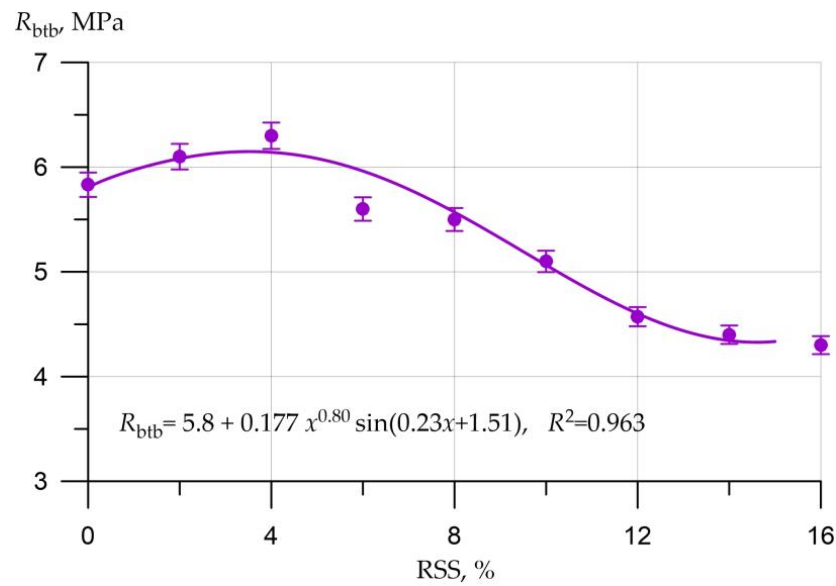


Figure 6. Consequences of investigational studies of the influence of local replacement of CA with RT seed shells on TS in twisting R_{btb} .

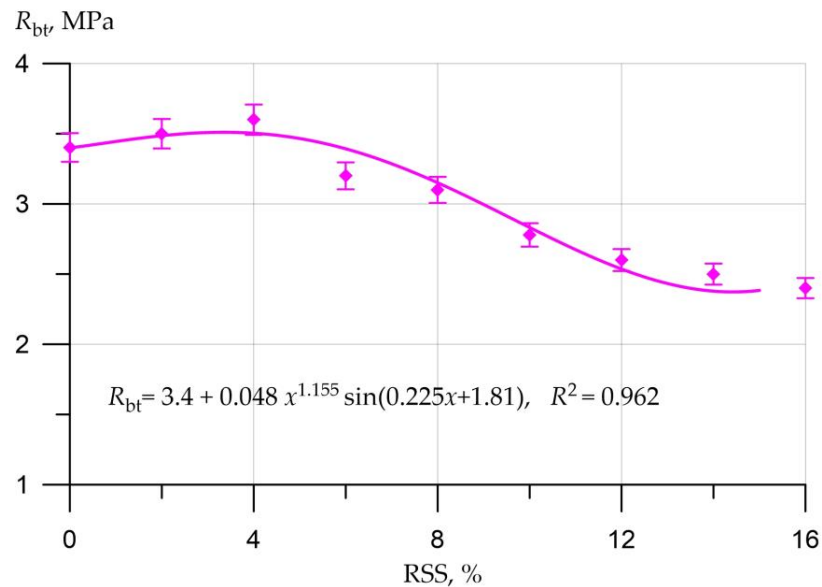


Figure 7. Results of investigational studies of the influence of local replacement of CA with RT seed shells on axial TS R_{bt} .

Figure 4 demonstrates that when coarse filler is replaced with RSS in the quantity of 2% and 4%, a gradual increase in CS from 49.4 MPa to 51.7 MPa is observed. However, when replacing bulk filler, starting from 6% and up to 16%, the reverse trend of change in CS is observed. The CS values were 46.3 MPa when replaced with RSS in the amount of 6% and 44.8 MPa, 40.9 MPa, 39.7 MPa, 38.1 MPa and 37.6 MPa when replaced in the amount of 8%, 10%, 12%, 14% and 16%, respectively. This can be explained by the denser packing created by the battered sandstone and the shells of the RT seeds.

The obtained experimental data have good convergence. The deviation of approximated and experimental data does not exceed 6%. The residual sum of squares is 6.87314. The coefficient of determination is $R^2 = 0.968$.

The dependence of cubic strength on RSS is well approximated by the formula

$$R_{b.cub} = 48.6 + 0.74x^{1.03} \sin(0.18x + 2.22), R^2 = 0.968 \tag{7}$$

where x is RSS, % and R^2 is the coefficient of determination.

The results of the experimental studies of CS (Figure 5), TS in twisting (Figure 6) and axial TS (Figure 7) with regard to the amount of RT seed shells are approximated by Equations (8)–(10):

$$R_b = 36.1 + 0.97 x^{0.88} \sin(0.23x + 1.66), R^2 = 0.935 \quad (8)$$

$$R_{btb} = 5.8 + 0.177 x^{0.80} \sin(0.23x + 1.51), R^2 = 0.963 \quad (9)$$

$$R_{bt} = 3.4 + 0.048 x^{1.155} \sin(0.225x + 1.81), R^2 = 0.962 \quad (10)$$

A large coefficient of determination indicates good agreement between the experimental data and the approximating theoretical function.

The trend in axial compressive strength, flexural TS and axial TS (Figures 5–7) is similar in nature to that of compressive strength. So, the maximum values of strengths in all cases are fixed at the amount of RSS 4%. With a further increase in the replacement of coarse filler with the shell of the seeds of the RT, a drop in strength features is observed.

Photos of the process of testing concrete samples for axial compression are shown in Figure 8.

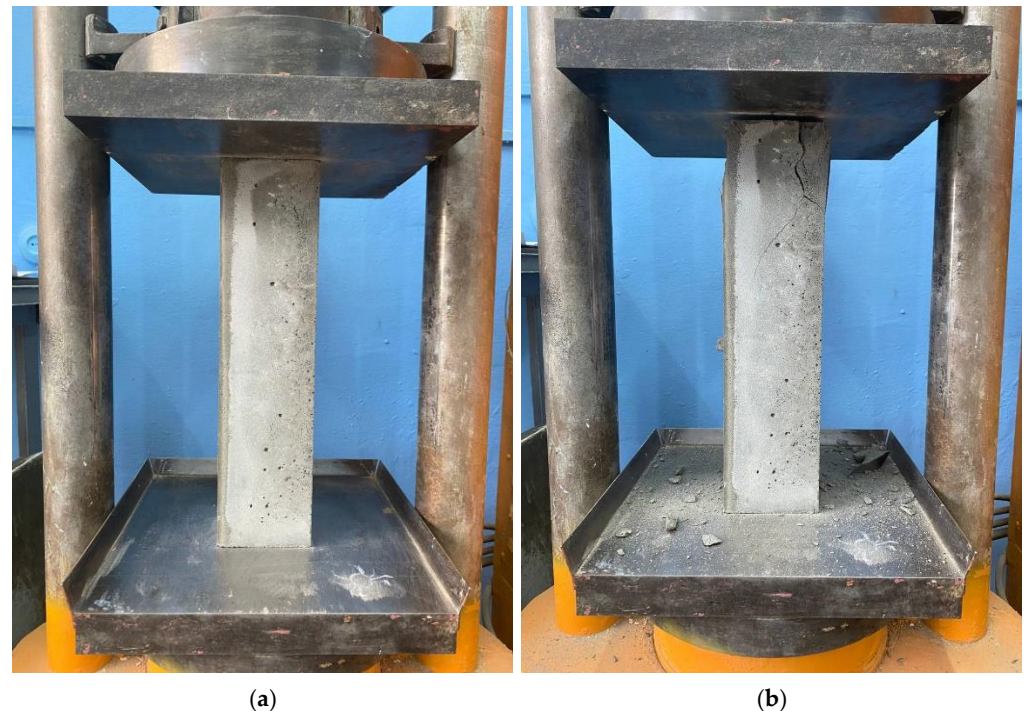


Figure 8. Axial compressive testing of concrete specimens: (a) initial phase of loading; (b) collapse phase.

Figures 9–11 show the study results of the influence of the ratio of replacement of CA with RT seed shells on the deformation features of concrete.

Figures 9 and 10 show that the nature of the change in ultimate strain is similar under axial compression and tension. Thus, when replacing coarse filler with the shells of seeds of an RT in the amount of 2% and 4%, a decrease in the values of limiting deformation is observed, and starting from 6%, an increase is noticeable. As for the modulus of elasticity, its maximum value was fixed at an amount of RSS of 4%, while when replacing coarse filler with RSS in an amount of 6% or more, a drop in the modulus of elasticity was observed.

Changes in the strength–strain features of concrete samples depending on the ratio of local replacement of CA with RT seed shells are presented in Table 2 and are denoted as a ratio associated with the control composition (without RSS).

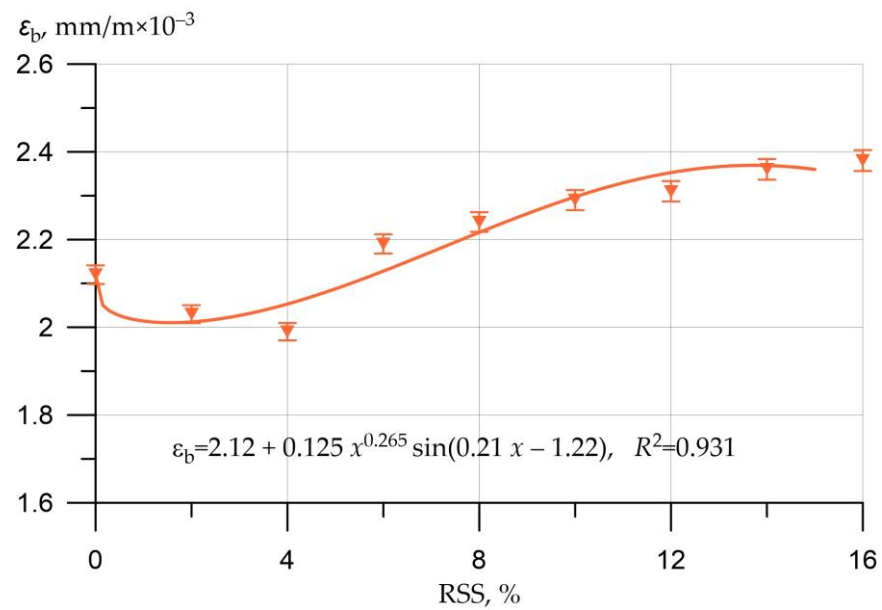


Figure 9. Results of investigational studies of the influence of local replacement of CA with RT seed shells on ultimate deformations under axial compression ϵ_b .

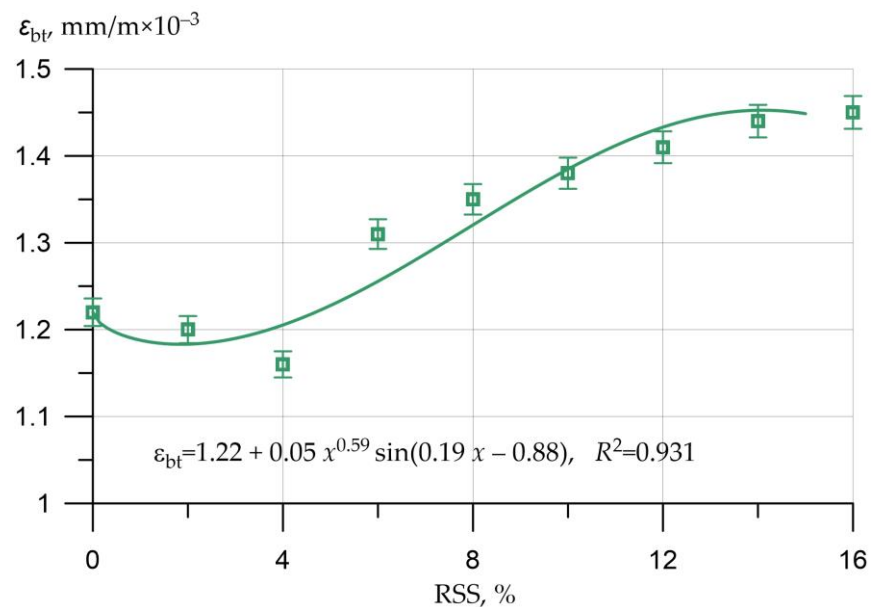


Figure 10. Results of investigational studies of the influence of local replacement of CA with RT seed shells on ultimate strains in axial tension ϵ_{bt} .

After analyzing the dependencies and data on variations in the features of concrete, as indicated in Table 2, we can conclude that the most effective is the local replacement of large mineral aggregate in concrete with a natural analogue in the form of RT seed shell in an amount of 4% by volume. This ratio of local replacement makes it possible to achieve maximum strength features. Therefore, the value of the CS was 51.7 MPa, the axial CS was 38.9 MPa, the TS in twisting was 6.3 MPa, and the axial TS was 3.6 MPa. It should be noted that the local replacement of CA with RT seed shells in an amount of 2% also contributes to an increase in strength features. When replacing coarse filler with 6% and 8% RSS, a contrary affiliation is detected in the form of a decrease in strength features. When replacing coarse aggregates at 10%, 12%, 14% and 16%, the strength decreased significantly and became much lower than the strength of the control composition.

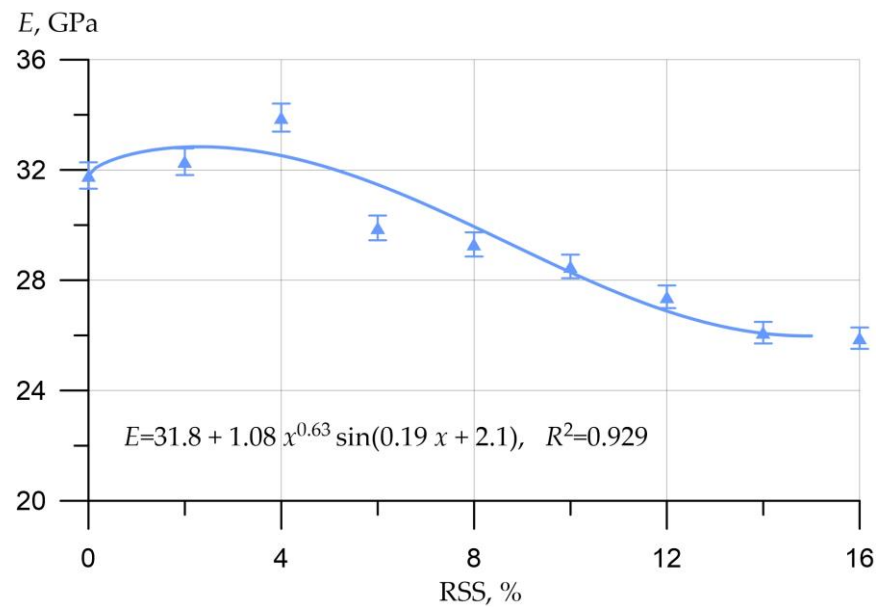


Figure 11. Results of investigational studies of the influence of local replacement of CA with RT seed shells on the elastic modulus E .

Table 2. Change in the strength–strain features of samples depending on the ratio of local replacement of CA with RT seed shells (Δ).

RSS, %	Δ , %						
	$R_{b,cub}$, MPa	R_b , MPa	R_{btb} , MPa	R_{bt} , MPa	ϵ_{bR} , mm/m $\times 10^{-3}$	ϵ_{btR} , mm/m $\times 10^{-4}$	E , GPa
0	0	0	0	0	0	0	0
2	2	5	5	3	−4	−2	2
4	6	8	8	6	−6	−5	7
6	−5	−6	−4	−6	3	7	−6
8	−8	−8	−6	−9	6	11	−8
10	−16	−19	−13	−18	8	13	−10
12	−18	−20	−22	−24	9	16	−14
14	−22	−24	−25	−27	11	18	−18
16	−23	−27	−26	−29	12	19	−19

Furthermore, following the test consequences, figures showing the compression “ $\epsilon_b - \sigma_b$ ” and tension “ $\epsilon_{bt} - \sigma_{bt}$ ” were made. Graphical curves of “stress–strain” are presented in Figures 12 and 13.

From the analysis of the concrete deformation diagrams representing local replacement of CA with the shells of RT seeds, the following assumptions can be made. The local replacement of CA with RT seed shells affects the deformation of the concrete in the following way: concretes with the replacement of large aggregates in the amount of 6%, 8%, 10%, 12%, 14% and 16% move up and to the right in the figure in comparison to the control sample.

The revealed picture of the change in the deformation properties of the obtained concretes is consistent with the picture of the change in their mechanical properties. That is, there is an ascending branch with a peak shift up and to the left for samples with a dosage of 4%, which have the highest mechanical properties. This is due to the highest strength of concrete of such samples and, accordingly, the lowest deformability. With a gradual increase in the content of vegetable aggregate in the body of the composite, the mechanical tensile strength of concrete somehow decreases, but at the same time its deformability increases, acquiring a more plastic character. Thus, the nature of the branch illustrating the

concrete deformation diagram in the descending part also changes. It becomes flatter, with a gradual shift of the peak of the diagram to the right and down.

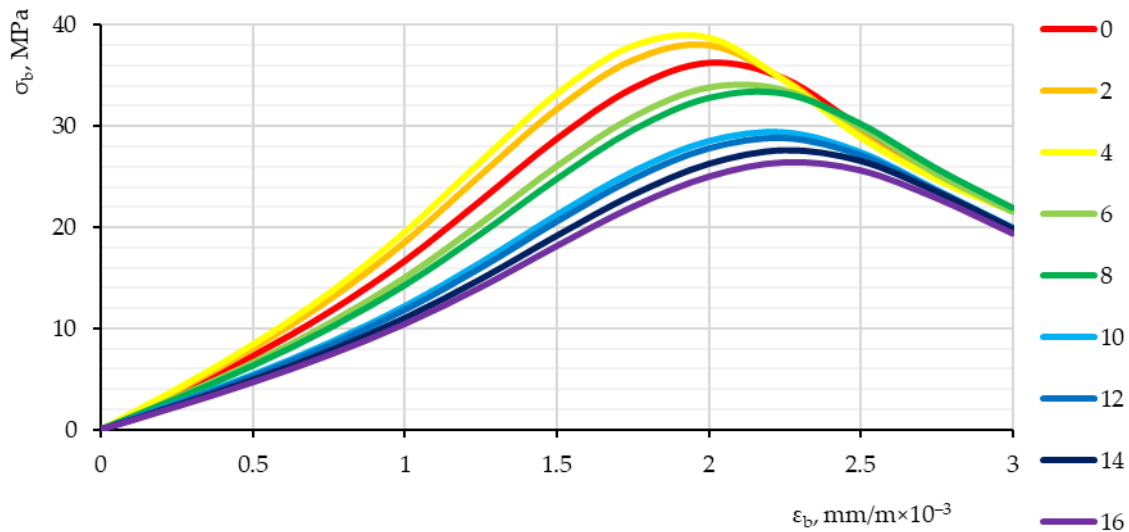


Figure 12. Stress–strain diagram under compression.

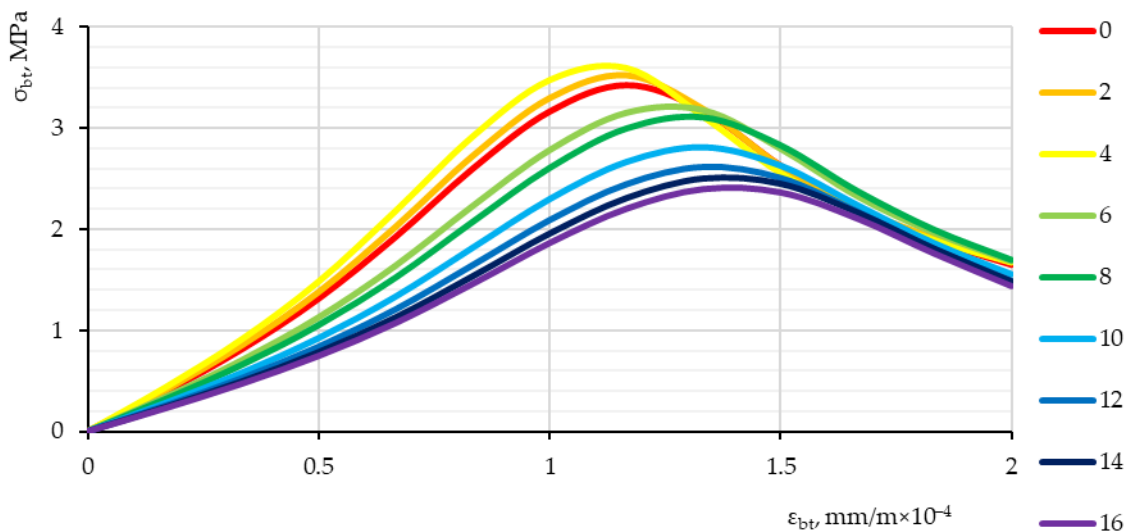
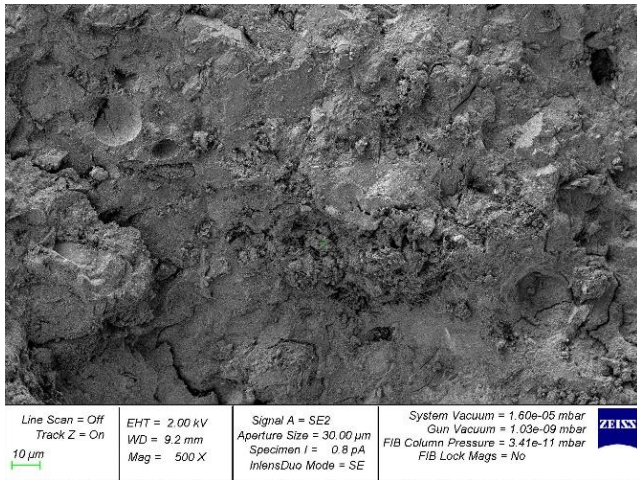


Figure 13. Tensile stress–strain diagram.

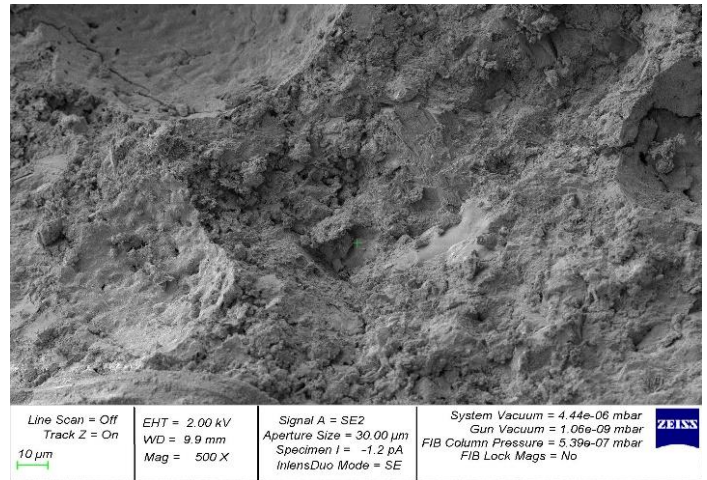
3.2. Investigation of the Microstructure of Hardened Concrete with Local Replacement of CA with RT Seed Shells

Figure 14 shows photos of the microstructure of hardened concrete with local replacement of CA with RT seed shells in an amount of 2–16% with a step of 2% by volume.

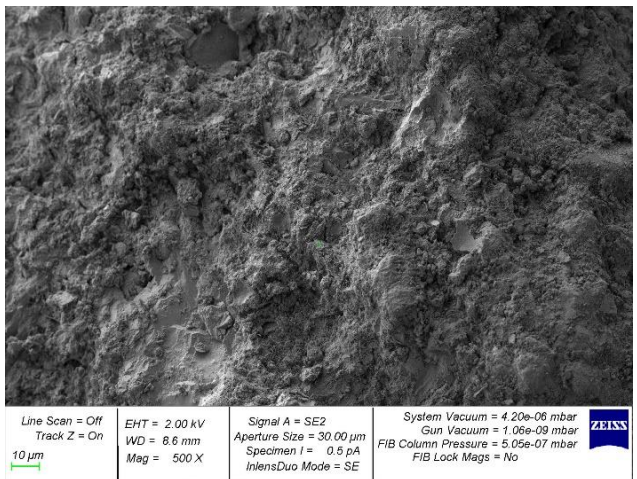
Figure 14 shows that the microstructure of hardened concrete samples with local replacement of CA with RT seed shells in the amount of 2% (Figure 14b), 4% (Figure 14c) and 6% (Figure 14c) is the most dense, with the least number of pores and microcracks compared with the microstructure of the control sample (Figure 14a) as well as samples with the replacement of coarse filler with RSS in an amount of more than 6% (Figure 14e–i), which is consistent with the results of experimental studies.



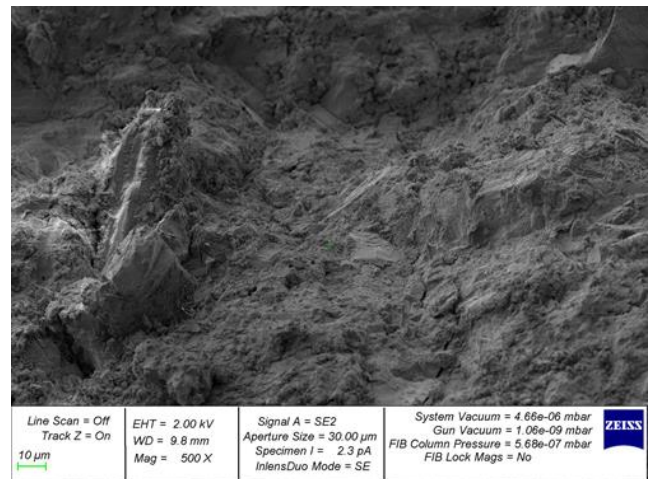
(a)



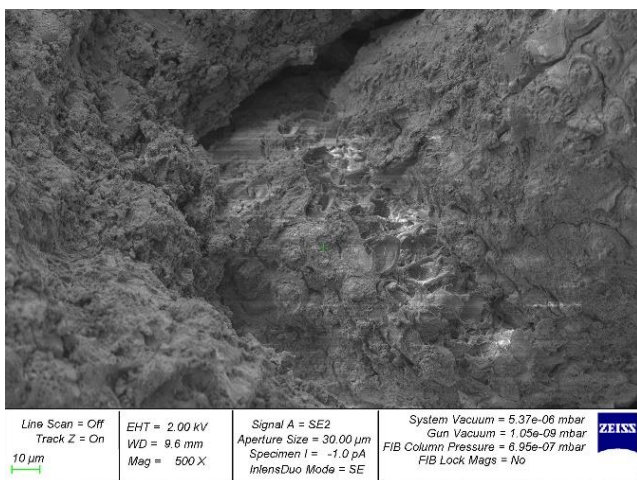
(b)



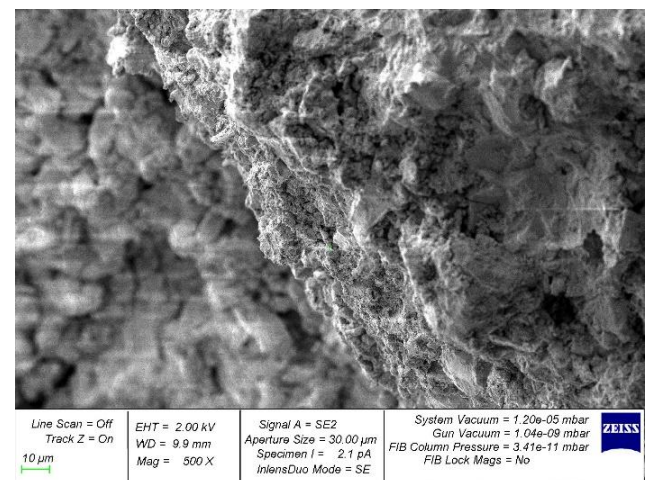
(c)



(d)



(e)



(f)

Figure 14. Cont.

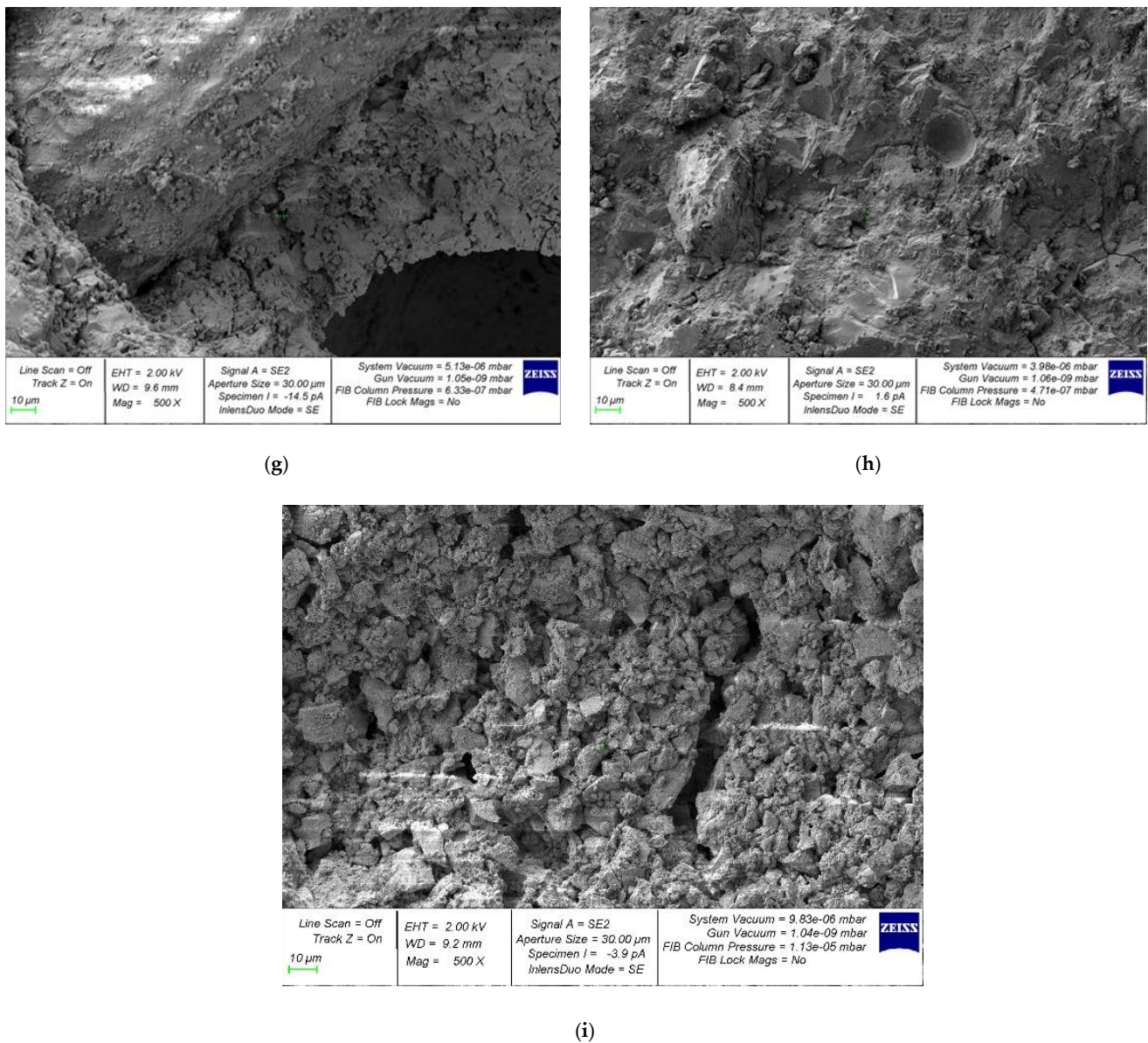


Figure 14. Photos of the microstructure of hardened concrete samples with local replacement of CA by RSS at (a) 0%; (b) 2%; (c) 4%; (d) 6%; (e) 8%; (f) 10%; (g) 12%; (h) 14%; (i) 16%.

The pattern of structure formation revealed at the micro level indicates a good compatibility of mineral and plant components in concrete, stabilization of crystallization centers at a high level, prevention of microstructural ruptures, and the absence of micro and macro cracks, which have a negative effect. Together with the high technological efficiency of the proposed method, a detailed examination of the pattern of microstructure formation fully meets the purpose of the study and confirms the working hypothesis.

4. Discussion

Previous studies in Malaysia on the use of RT seed shells as a CA for concrete, after being processed by crushing to a specific fraction, were mainly aimed at studying the mechanical properties of this concrete. Strength features were determined, which directly reflected the ability of such concrete to absorb mechanical loads according to the criterion of compressive strength. However, this indicates that there is a serious scientific deficit in the study of the deformation features of concrete using RT seed shells; structural studies are needed at the micro level to confirm the effectiveness of the proposed method. Thus,

this study fills this scientific gap and provides an empirical basis for subsequent research. However, the empirical basis alone is not enough to evaluate the influence. This can be explained in terms of microstructure, using SEM analysis. With the help of an electron microscope, it was possible to photograph fragments of concrete located near the interface between the cement–sand mortar and RSS phases. Due to the fact that the cement–sand mortar acts as a matrix in the resulting composite, and the shell of the RT seeds, unlike traditional stone aggregates, acts as a filler, but at the same time adds a damping, softening influence, we evaluated structural changes using a microscope. In terms of microcracking, it can be seen that the concrete structure is as homogeneous as possible. On average, there is no cracking on the studied fragments. There are no gaps between the cement–sand stone and the shell of the RT seeds due to the fact that the shell has some roughness and a good level of adhesion to the matrix. Thus, at the microstructural level, the expediency of introducing the RT seed shell as an aggregate for concrete is confirmed.

The nature of structure formation, the planned strength gain of concrete, as well as the changed deformation features indicate that the resulting concrete is promising for use, for example, in those structures that demand not only compressive strength but also twisting strength (floor and road structures with low load). That is, such concrete has a number of advantages compared to its counterpart with simple stone aggregates. There is a damping phenomenon during its operation, the elastic features are improved in general, the deformability changes, and the nature of the “stress–strain” diagram changes. Thus, such concrete is promising for use in certain products and structures.

The best values for the strength features and the densest structure of the hardened cement paste were established when replacing CA with 4% RSS by total volume. With regard to the maximum allowable ratio of replacement of aggregate with shells, this limit is fixed at around 8%. A further rise in the ratio of replacement of coarse filler leads to a significant decrease in strength features, of more than 10%. The same is true for the modulus of elasticity. At RSS dosages of 6% and 8%, the drop in strength features is not as critical, which makes it possible to further use these concrete compositions in practice.

Thus, the most important parameter in the creation of new concretes including mineral and vegetable components is the percentage of these two parts. In particular, the nature of the effectiveness of the partial replacement of traditional filler with vegetable (RSS) has both an ascending branch and a descending branch. Reaching its optimum, the content of the plant component subsequently increases to a state of supersaturation, which not only stops the growth of the mechanical characteristics of the composite, but also leads to a systematic decrease. Thus, we experimentally determined and proved the rational range of values of this ratio.

The contribution of the research presented in this article to science and practice can be fully appreciated only by comparing the work done with the work of other authors. Despite the small number of studies, it is important to compare the study in terms of methodological, technological, research and analytical approach and in terms of practical applicability of the study.

Considering the study from the point of view of the methodological aspect, it can be noted that for the first time, a comprehensive approach was provided, based on a detailed study of the parameters of the employed by-product of the agricultural industry: the shell of the seeds of the RT. The study of the raw materials employed was carried out, and then the dependencies between the final strength and deformation features of the resulting concrete were identified with the local replacement of CA with the shell of RT seeds.

Considering our study from the point of view of the technological approach, we can conclude that our article differs in that we describe the methods for obtaining and processing agricultural by-products, their disposal, and the technological and prescription factors that affect the process of manufacturing concrete compositions with local replacement of CA with a natural analogue. This is characteristically different from previous studies [40,41].

Additionally, it should be noted that the proposed rubber tree seed shell aggregate has a number of advantages compared to dense rock aggregates and some porous aggregates.

This is expressed in a decrease in the total mass of concrete structures while maintaining a good degree of adhesion of the aggregate to the hardened cement paste and the absence of significant defect formation at the phase boundaries. In addition, the applied aggregate itself is noted in some studies for high physical characteristics, allowing it to remain at a competitive level. Thus, in refs. [40,41], data are given on its water absorption from 24 to 30%, which corresponds to the expediency of its use in concrete, taking into account its advantages.

As part of the research aspect, we have applied various methods:

- Comparison of test results of concrete with local replacement of CA with the results achieved for the control composition;
- A series of mechanical experiments;
- Numerical processing, including performing mathematical calculations to predict consequences and determine mathematical dependencies.

From the analytics point of view, the dependencies of the strength and deformation features on the initial components were determined. Therefore, the article is both a scientific study performed with the aim of obtaining new aspects and developing existing ideas of concrete with local replacement of large aggregates with by-products of the agricultural industry, and is of practical importance in that it allows solving the actual problems in the construction and agricultural industries, which are the consumers and suppliers of rapidly renewable, high-quality raw materials collected in large volumes.

The strength features and other quantifiable indicators of the resulting concrete were attained with the local replacement of CA with a natural analogue. Therefore, refs. [40,41] found increases in strength features of concrete from 1% to 3% due to the limited replacement of CA with the shell of RT seeds. Our recommendations made it possible to increase the strength of concrete by up to 6%. The “stress–strain” diagrams based on the results of the composition achieved in this article made it possible to identify a slight improvement in the deformation features. The weight of the resulting compositions and their cost also decreased. Therefore, the methods employed resulted in an improvement in comparison with the works by other authors [40,41].

Therefore, the article is not only of a functional technical nature but also is aimed at achieving financial productivity.

5. Conclusions

- (1) Improvements in concrete performance were observed when CA was replaced by volume with RT seed shells at a rate of 4%. The strength values at this RSS dosage were CS—51.7 MPa, axial CS—38.9 MPa, axial TS—3.6 MPa, TS in twisting—6.3 MPa, and the values of deformations during compression and tension were respectively equal to $1.99 \text{ mm/m} \times 10^{-3}$ and $1.16 \text{ mm/m} \times 10^{-4}$. The modulus of elasticity was 33.9 GPa.
- (2) The increase in the strength of concrete, as well as changes in deformability, according to the results of our examination of the “stress–strain” figures were: for CS 6%, for axial CS 8%, for axial TS 6% and for TS in twisting 8%
- (3) Changes in deformability included an increase in the elastic modulus of 7%, and a reduction in strains under compression of 6% and strains under tension of 5%.
- (4) The microstructure of hardened concrete samples with partial replacement of CA with RT seed shells in the amount of 2%, 4% and 6% is the most dense, with the fewest pores and microcracks in comparison with the structure of the sample of the control composition, as well as samples with the replacement of CA with RT seed shells in the amount of more than 6%.
- (5) According to our preliminary estimates, the expedient and effective replacement of CA with RT seed shells leads to a reduction in the consumption of mineral CA by up to 8%.
- (6) The achieved results established good compatibility of data and the opportunity of analysis of the technology in manufacturing situations. Future research is planned to

study the influence of replacing CA with RT seed shells on the physical features of concrete, such as thermal insulation and resistance to cyclic influences, as well as its cost and the development of a cost-effective production technology.

Author Contributions: Conceptualization, S.A.S., E.M.S., A.N.B. and A.A.S.; methodology, S.A.S., E.M.S., Y.O.Ö., C.A. and V.V.; software, S.A.S., E.M.S., A.N.B., Y.O.Ö. and C.A.; validation, A.A.S., S.A.S., E.M.S. and A.N.B.; formal analysis, A.E., S.A.S. and E.M.S.; investigation, S.A.S., E.M.S., A.N.B., Y.O.Ö., C.A. and B.M.; resources, B.M.; data curation, S.A.S., E.M.S. and C.A.; writing—original draft preparation, S.A.S., Y.O.Ö., C.A., M.K., E.M.S. and A.N.B.; writing—review and editing, M.K., S.A.S., E.M.S. and A.N.B.; visualization, V.V., S.A.S., E.M.S. and A.N.B.; supervision, B.M.; project administration, B.M.; funding acquisition, A.N.B. and B.M. All authors have read and agreed to the published version of the manuscript.

Funding: This research received no external funding.

Institutional Review Board Statement: Not applicable.

Informed Consent Statement: Not applicable.

Data Availability Statement: The study did not report any data.

Acknowledgments: The authors would like to acknowledge the administration of Don State Technical University for their resources and financial support.

Conflicts of Interest: The authors declare no conflict of interest.

Abbreviations

CA	coarse aggregate
CS	compressive strength
RCS	reinforced concrete structure
RSS	rubber seed shell
RT	rubber tree
TS	tensile strength

References

1. Aksoylu, C.; Özkılıç, Y.O.; Hadzima-Nyarko, M.; Işık, E.; Arslan, M.H. Investigation on Improvement in Shear Performance of Reinforced-Concrete Beams Produced with Recycled Steel Wires from Waste Tires. *Sustainability* **2022**, *14*, 13360. [[CrossRef](#)]
2. Çelik, A.İ.; Özkılıç, Y.O.; Zeybek, Ö.; Özdöner, N.; Tayeh, B.A. Performance Assessment of Fiber-Reinforced Concrete Produced with Waste Lathe Fibers. *Sustainability* **2022**, *14*, 11817. [[CrossRef](#)]
3. Abbas, S.; Ishaq, M.A.A.; Kazmi, S.M.S.; Munir, M.J.; Ali, S. Investigating the Behavior of Waste Alumina Powder and Nylon Fibers for Eco-Friendly Production of Self-Compacting Concrete. *Materials* **2022**, *15*, 4515. [[CrossRef](#)] [[PubMed](#)]
4. Joyklad, P.; Yooprasertchai, E.; Rahim, A.; Ali, N.; Chaiyasarn, K.; Hussain, Q. Sustainable and Low-Cost Hemp FRP Composite Confinement of B-Waste Concrete. *Sustainability* **2022**, *14*, 7673. [[CrossRef](#)]
5. Karalar, M.; Özkılıç, Y.O.; Deifalla, A.F.; Aksoylu, C.; Arslan, M.H.; Ahmad, M.; Sabri, M.M.S. Improvement in Bending Performance of Reinforced Concrete Beams Produced with Waste Lathe Scraps. *Sustainability* **2022**, *14*, 12660. [[CrossRef](#)]
6. Oupparamong, T.; Gunun, N.; Tamkhonburee, C.; Khejornsart, P.; Kaewpila, C.; Kesorn, P.; Kimprasit, T.; Cherdthong, A.; Wanapat, M.; Polyorach, S.; et al. Fermented Rubber Seed Kernel with Yeast in the Diets of Tropical Lactating Dairy Cows: Effects on Feed Intake, Hematology, Microbial Protein Synthesis, Milk Yield and Milk Composition. *Vet. Sci.* **2022**, *9*, 360. [[CrossRef](#)]
7. Gunun, N.; Oupparamong, T.; Khejornsart, P.; Cherdthong, A.; Wanapat, M.; Polyorach, S.; Kaewpila, C.; Kang, S.; Gunun, P. Effects of Rubber Seed Kernel Fermented with Yeast on Feed Utilization, Rumen Fermentation and Microbial Protein Synthesis in Dairy Heifers. *Fermentation* **2022**, *8*, 288. [[CrossRef](#)]
8. Jirimali, H.; Singh, J.; Boddula, R.; Lee, J.-K.; Singh, V. Nano-Structured Carbon: Its Synthesis from Renewable Agricultural Sources and Important Applications. *Materials* **2022**, *15*, 3969. [[CrossRef](#)]
9. Liu, J.; Zhao, L.; Cai, H.; Zhao, Z.; Wu, Y.; Wen, Z.; Yang, P. Antioxidant and Anti-Inflammatory Properties of Rubber Seed Oil in Lipopolysaccharide-Induced RAW 267.4 Macrophages. *Nutrients* **2022**, *14*, 1349. [[CrossRef](#)]
10. Ramli, S.F.; Aziz, H.A.; Omar, F.M.; Yusoff, M.S.; Halim, H.; Kamaruddin, M.A.; Ariffin, K.S.; Hung, Y.-T. Influence of Particle Size and Zeta Potential in Treating Highly Coloured Old Landfill Leachate by Tin Tetrachloride and Rubber Seed. *Int. J. Environ. Res. Public Health* **2022**, *19*, 3016. [[CrossRef](#)] [[PubMed](#)]
11. Šourková, M.; Adamcová, D.; Vavřková, M.D. The Influence of Microplastics from Ground Tyres on the Acute, Subchronical Toxicity and Microbial Respiration of Soil. *Environments* **2021**, *8*, 128. [[CrossRef](#)]

12. Kumar, S.S.; Rajan, K.; Mohanavel, V.; Ravichandran, M.; Rajendran, P.; Rashedi, A.; Sharma, A.; Khan, S.A.; Afzal, A. Combustion, Performance, and Emission Behaviors of Biodiesel Fueled Diesel Engine with the Impact of Alumina Nanoparticle as an Additive. *Sustainability* **2021**, *13*, 12103. [[CrossRef](#)]
13. Ramli, S.F.; Aziz, H.A.; Omar, F.M.; Yusoff, M.S.; Halim, H.; Kamaruddin, M.A.; Ariffin, K.S.; Hung, Y.-T. Reduction of COD and Highly Coloured Mature Landfill Leachate by Tin Tetrachloride with Rubber Seed and Polyacrylamide. *Water* **2021**, *13*, 3062. [[CrossRef](#)]
14. Nun-Anan, P.; Hayichelaeh, C.; Boonkerd, K. Effect of a Natural Processing Aid on the Properties of Acrylonitrile-Butadiene Rubber: Study on Soybean Oil Fatty Acid from Seed Crop. *Polymers* **2021**, *13*, 3459. [[CrossRef](#)] [[PubMed](#)]
15. Hu, Y.; Zhu, G.; Zhang, J.; Huang, J.; Yu, X.; Shang, Q.; An, R.; Liu, C.; Hu, L.; Zhou, Y. Rubber Seed Oil-Based UV-Curable Polyurethane Acrylate Resins for Digital Light Processing (DLP) 3D Printing. *Molecules* **2021**, *26*, 5455. [[CrossRef](#)] [[PubMed](#)]
16. Cujbescu, D.; Găgeanu, I.; Persu, C.; Matache, M.; Vlăduț, V.; Voicea, I.; Paraschiv, G.; Biriș, S.Ș.; Ungureanu, N.; Voicu, G.; et al. Simulation of Sowing Precision in Laboratory Conditions. *Appl. Sci.* **2021**, *11*, 6264. [[CrossRef](#)]
17. Mokti, N.; Borhan, A.; Zaine, S.N.A.; Mohd Zaid, H.F. Development of Rubber Seed Shell-Activated Carbon Using Impregnated Pyridinium-Based Ionic Liquid for Enhanced CO₂ Adsorption. *Processes* **2021**, *9*, 1161. [[CrossRef](#)]
18. Wang, J.; Xu, C.; Xu, Y.; Wang, Z.; Qi, X.; Wang, J.; Zhou, W.; Tang, H.; Wang, Q. Influencing Factors Analysis and Simulation Calibration of Restitution Coefficient of Rice Grain. *Appl. Sci.* **2021**, *11*, 5884. [[CrossRef](#)]
19. Borhan, A.; Yusuf, S. Activation of Rubber-Seed Shell Waste by Malic Acid as Potential CO₂ Removal: Isotherm and Kinetics Studies. *Materials* **2020**, *13*, 4970. [[CrossRef](#)] [[PubMed](#)]
20. Tang, J.; Zhang, J.; Lu, J.; Huang, J.; Zhang, F.; Hu, Y.; Liu, C.; An, R.; Miao, H.; Chen, Y.; et al. Preparation and Properties of Plant-Oil-Based Epoxy Acrylate-Like Resins for UV-Curable Coatings. *Polymers* **2020**, *12*, 2165. [[CrossRef](#)]
21. Okubo, T.; Ikeda, T.; Saruta, J.; Tsukimura, N.; Hirota, M.; Ogawa, T. Compromised Epithelial Cell Attachment after Polishing Titanium Surface and Its Restoration by UV Treatment. *Materials* **2020**, *13*, 3946. [[CrossRef](#)] [[PubMed](#)]
22. Medeiros, A.M.S.; Bourgeat-Lami, E.; McKenna, T.F.L. Styrene-Butadiene Rubber by Miniemulsion Polymerization Using In Situ Generated Surfactant. *Polymers* **2020**, *12*, 1476. [[CrossRef](#)]
23. Marques, L.; Martinez, G.; Guidelli, É.; Tamashiro, J.; Segato, R.; Payão, S.L.M.; Baffa, O.; Kinoshita, A. Performance on Bone Regeneration of a Silver Nanoparticle Delivery System Based on Natural Rubber Membrane NRL-AgNP. *Coatings* **2020**, *10*, 323. [[CrossRef](#)]
24. Falowo, O.A.; Ojumu, T.V.; Perea, O.; Betiku, E. Sustainable Biodiesel Synthesis from Honne-Rubber-Neem Oil Blend with a Novel Mesoporous Base Catalyst Synthesized from a Mixture of Three Agrowastes. *Catalysts* **2020**, *10*, 190. [[CrossRef](#)]
25. Sihombing, J.L.; Gea, S.; Wirjosentono, B.; Agusnar, H.; Pulungan, A.N.; Herlinawati, H.; Yusuf, M.; Hutapea, Y.A. Characteristic and Catalytic Performance of Co and Co-Mo Metal Impregnated in Sarulla Natural Zeolite Catalyst for Hydrocracking of MEFA Rubber Seed Oil into Biogasoline Fraction. *Catalysts* **2020**, *10*, 121. [[CrossRef](#)]
26. Borhan, A.; Yusup, S.; Lim, J.W.; Show, P.L. Characterization and Modelling Studies of Activated Carbon Produced from Rubber-Seed Shell Using KOH for CO₂ Adsorption. *Processes* **2019**, *7*, 855. [[CrossRef](#)]
27. Romuli, S.; Karaj, S.; Müller, J. Physical Properties of *Jatropha curcas* L. Fruits and Seeds with Respect to Their Maturity Stage. *Appl. Sci.* **2019**, *9*, 1802. [[CrossRef](#)]
28. Winoto, V.; Yoswathana, N. Optimization of Biodiesel Production Using Nanomagnetic CaO-Based Catalysts with Subcritical Methanol Transesterification of Rubber Seed Oil. *Energies* **2019**, *12*, 230. [[CrossRef](#)]
29. Adam, I.K.; Abdul Aziz, A.R.; Heikal, M.R.; Yusup, S.; Firmansyah; Ahmad, A.S.; Zainal Abidin, E.Z. Performance and Emission Analysis of Rubber Seed, Palm, and Their Combined Blend in a Multi-Cylinder Diesel Engine. *Energies* **2018**, *11*, 1522. [[CrossRef](#)]
30. Abbas, S.N.; Qureshi, M.I.; Abid, M.M.; Tariq, M.A.U.R.; Ng, A.W.M. An Investigation of Mechanical Properties of Concrete by Applying Sand Coating on Recycled High-Density Polyethylene (HDPE) and Electronic-Wastes (E-Wastes) Used as a Partial Replacement of Natural Coarse Aggregates. *Sustainability* **2022**, *14*, 4087. [[CrossRef](#)]
31. Khanzada, F.A.; Nazir, K.; Ishtiaq, M.; Javed, M.F.; Kashif-ur-Rehman, S.; Aslam, F.; Musarat, M.A.; Usanova, K.I. Concrete by Preplaced Aggregate Method Using Silica Fume and Polypropylene Fibres. *Materials* **2022**, *15*, 1997. [[CrossRef](#)] [[PubMed](#)]
32. Ahmad, F.; Jamal, A.; Mazher, K.M.; Umer, W.; Iqbal, M. Performance Evaluation of Plastic Concrete Modified with E-Waste Plastic as a Partial Replacement of Coarse Aggregate. *Materials* **2022**, *15*, 175. [[CrossRef](#)]
33. Ahmed, S.; Mahaini, Z.; Abed, F.; Mannan, M.A.; Al-Samarai, M. Microstructure and Mechanical Property Evaluation of Dune Sand Reactive Powder Concrete Subjected to Hot Air Curing. *Materials* **2022**, *15*, 41. [[CrossRef](#)] [[PubMed](#)]
34. Diotti, A.; Cominoli, L.; Plizzari, G.; Sorlini, S. Experimental Evaluation of Recycled Aggregates, Washing Water and Cement Sludge Recovered from Returned Concrete. *Appl. Sci.* **2022**, *12*, 36. [[CrossRef](#)]
35. Nafees, A.; Javed, M.F.; Khan, S.; Nazir, K.; Farooq, F.; Aslam, F.; Musarat, M.A.; Vatin, N.I. Predictive Modeling of Mechanical Properties of Silica Fume-Based Green Concrete Using Artificial Intelligence Approaches: MLPNN, ANFIS, and GEP. *Materials* **2021**, *14*, 7531. [[CrossRef](#)]
36. Raja, K.C.P.; Thianarasu, I.; Elkoth, M.A.; Ansari, K.; Saleel, C.A. Shrinkage Study and Strength Aspects of Concrete with Foundry Sand and Coconut Shell as a Partial Replacement for Coarse and Fine Aggregate. *Materials* **2021**, *14*, 7420. [[CrossRef](#)]
37. Kočí, V.; Kočí, J.; Fořt, J.; Fiala, L.; Šál, J.; Hager, I.; Černý, R. Utilization of Crushed Pavement Blocks in Concrete: Assessment of Functional Properties and Environmental Impacts. *Materials* **2021**, *14*, 7361. [[CrossRef](#)] [[PubMed](#)]

38. Garcia-Troncoso, N.; Xu, B.; Probst-Pesantez, W. Development of Concrete Incorporating Recycled Aggregates, Hydrated Lime and Natural Volcanic Pozzolan. *Infrastructures* **2021**, *6*, 155. [CrossRef]
39. Taqa, A.A.; Al-Ansari, M.; Taha, R.; Senouci, A.; Al-Zubi, G.M.; Mohsen, M.O. Performance of Concrete Mixes Containing TBM Muck as Partial Coarse Aggregate Replacements. *Materials* **2021**, *14*, 6263. [CrossRef]
40. Muthusamy, K.; Nordin, N.; Vesuvapateran, G.; Ali, M.; Annual, N.M.; Harun, H.; Ullap, H. Exploratory Study of Rubber Seed Shell as Partial Coarse Aggregate Replacement in Concrete. *Res. J. Appl. Sci. Eng. Technol.* **2014**, *7*, 1199–1202. [CrossRef]
41. Raksritong, D.; Tonnyapopas, D.; Taweepreda, W.; Masniyom, M. Green Lightweight Concrete Made from Natural Para Rubber Product. *Key Eng. Mater.* **2013**, *594–595*, 460–464.
42. Moradi, N.; Tavana, M.H.; Habibi, M.R.; Amiri, M.; Moradi, M.J.; Farhangi, V. Predicting the Compressive Strength of Concrete Containing Binary Supplementary Cementitious Material Using Machine Learning Approach. *Materials* **2022**, *15*, 5336. [CrossRef]
43. Ahmad, J.; Zhou, Z.; Majidi, A.; Alqurashi, M.; Deifalla, A.F. Overview of Concrete Performance Made with Waste Rubber Tires: A Step toward Sustainable Concrete. *Materials* **2022**, *15*, 5518. [CrossRef]
44. Zadehmohamad, M.; Bazaz, J.B.; Riahipour, R.; Farhangi, V. Physical modeling of the long-term behavior of integral abutment bridge backfill reinforced with tire-rubber. *Geo-Engineering* **2021**, *12*, 36. [CrossRef]
45. Han, Q.; Wang, N.; Zhang, J.; Yu, J.; Hou, D.; Dong, B. Experimental and Computational Study on Chloride Ion Transport and Corrosion Inhibition Mechanism of Rubber Concrete. *Constr. Build. Mater.* **2021**, *268*, 121105. [CrossRef]
46. Su, D.; Pang, J.; Huang, X. Experimental Study on the Influence of Rubber Content on Chloride Salt Corrosion Resistance Performance of Concrete. *Materials* **2021**, *14*, 4706. [CrossRef] [PubMed]
47. Roychand, R.; Gravina, R.J.; Zhuge, Y.; Ma, X.; Mills, J.E.; Youssef, O. Practical Rubber Pre-Treatment Approach for Concrete Use—An Experimental Study. *J. Compos. Sci.* **2021**, *5*, 143. [CrossRef]
48. Schmidt, M.; Fehling, E.; Geisenhanslüke, C. Ultra High Performance Concrete (UHPC). In Proceedings of the International Symposium on Ultra High Performance Concrete, Kassel, Germany, 13–15 September 2004; University of Kassel; 884p. Available online: <https://www.uni-kassel.de/upress/online/frei/978-3-89958-086-0.volltext.frei> (accessed on 15 November 2022).
49. Mubarik, S.; Qureshi, N.; Sattar, Z.; Shaheen, A.; Kalsoom, A.; Imran, M.; Hanif, F. Synthetic Approach to Rice Waste-Derived Carbon-Based Nanomaterials and Their Applications. *Nanomanufacturing* **2021**, *1*, 109–159. [CrossRef]
50. Beskopylny, A.N.; Stel'makh, S.A.; Shcherban', E.M.; Mailyan, L.R.; Meskhi, B.; Smolyanichenko, A.S.; Beskopylny, N. High-Performance Concrete Nanomodified with Recycled Rice Straw Biochar. *Appl. Sci.* **2022**, *12*, 5480. [CrossRef]
51. Shcherban', E.M.; Stel'makh, S.A.; Beskopylny, A.N.; Mailyan, L.R.; Meskhi, B.; Varavka, V.; Beskopylny, N.; El'shaeva, D. Enhanced Eco-Friendly Concrete Nano-Change with Eggshell Powder. *Appl. Sci.* **2022**, *12*, 6606. [CrossRef]
52. Beskopylny, A.N.; Stel'makh, S.A.; Shcherban', E.M.; Mailyan, L.R.; Meskhi, B.; Shilov, A.A.; Beskopylny, N.; Chernil'nik, A. Enhanced Performance of Concrete Dispersedly Reinforced with Sisal Fibers. *Appl. Sci.* **2022**, *12*, 9102. [CrossRef]
53. Beskopylny, A.N.; Stel'makh, S.A.; Shcherban', E.M.; Mailyan, L.R.; Meskhi, B.; Smolyanichenko, A.S.; Varavka, V.; Beskopylny, N.; Dotsenko, N. Influence of Electromagnetic Activation of Cement Paste and Nano-Modification by Rice Straw Biochar on the Structure and Characteristics of Concrete. *J. Compos. Sci.* **2022**, *6*, 268. [CrossRef]
54. GOST 18105 Concretes. Rules for Control and Assessment of Strength. Available online: <https://docs.cntd.ru/document/1200164028> (accessed on 14 October 2022).
55. GOST 10180 Concretes. Methods for Strength Determination Using Reference Specimens. Available online: <https://docs.cntd.ru/document/1200100908> (accessed on 14 October 2022).
56. GOST 24452 Concretes. Methods of Prismatic, Compressive Strength, Modulus of Elasticity and Poisson's Ratio Determination. Available online: <https://docs.cntd.ru/document/9056198> (accessed on 14 October 2022).
57. Beskopylny, A.N.; Stel'makh, S.A.; Shcherban', E.M.; Mailyan, L.R.; Meskhi, B.; El'shaeva, D.; Varavka, V. Developing Environmentally Sustainable and Cost-Effective Geopolymer Concrete with Improved Characteristics. *Sustainability* **2021**, *13*, 13607. [CrossRef]
58. Beskopylny, A.N.; Stel'makh, S.A.; Shcherban', E.M.; Mailyan, L.R.; Meskhi, B. Nano modifying additive micro silica influence on integral and differential characteristics of vibrocentrifuged concrete. *J. Build. Eng.* **2022**, *51*, 104235. [CrossRef]
59. Beskopylny, A.N.; Shcherban', E.M.; Stel'makh, S.A.; Mailyan, L.R.; Meskhi, B.; El'shaeva, D. The Influence of Composition and Recipe Dosage on the Strength Characteristics of New Geopolymer Concrete with the Use of Stone Flour. *Appl. Sci.* **2022**, *12*, 613. [CrossRef]
60. Shcherban', E.M.; Stel'makh, S.A.; Beskopylny, A.; Mailyan, L.R.; Meskhi, B.; Shuyskiy, A. Improvement of Strength and Strain Characteristics of Lightweight Fiber Concrete by Electromagnetic Activation in a Vortex Layer Apparatus. *Appl. Sci.* **2022**, *12*, 104. [CrossRef]